Reaction Mechanisms

DOI: 10.1002/anie.201400956

Three Roles for the Fluoride Ion in Palladium-Catalyzed Hiyama Reactions: Transmetalation of $[ArPdFL_2]$ by $Ar'Si(OR)_3$**

Christian Amatore, Laurence Grimaud,* Gaëtan Le Duc, and Anny Jutand**

***Abstract:** From the kinetic data on the transmetalation/reductive elimination in fluoride-promoted Hiyama reactions, obtained using electrochemical techniques, it has been established that fluoride ions play three roles. F^- reacts with trans-$[ArPdBrL_2]$ ($L = PPh_3$) to form trans-$[ArPdFL_2]$, which reacts with $Ar'Si(OMe)_3$ in the rate-determining transmetalation, whereas trans-$[ArPdBrL_2]$ does not react with $Ar'Si(OMe)_3$. F^- reacts with $Ar'Si(OMe)_3$ to deliver the unreactive silicate $Ar'SiF(OMe)_3^-$, thus leading to two antagonistic kinetic effects. In addition, F^- catalyzes the reductive elimination from intermediate trans-$[ArPdAr'L_2]$.*

The palladium-catalyzed Hiyama reactions between arylhalides and arylsilanes $Ar'Si$ [$Si = Si(OR)_3$, $SiRF_2$, SiF_3] are promoted by fluoride ions. They are often performed at high temperatures even with aryl iodides (Scheme 1).[1,2]

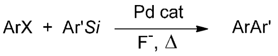

Scheme 1. Hiyama reactions promoted by fluoride ions.

The postulated mechanism of the Hiyama reaction involving $Ar'SiRF_2$ predicted a transmetalation of $[ArPdXL_2]$ (formed in the oxidative addition of ArX to $[Pd^0L_4]$) with the silicate $Ar'SiRF_3^-$, thus leading to $[ArPdAr'L_2]$ which generates ArAr' and $[Pd^0L_2]$.[2a] A transition state involving a Pd–F bond was also proposed.[2b] DFT calculations on the model reaction of $CH_2{=}CH{-}I$ with $CH_2{=}CH{-}SiMe_3$ in the presence of F^- ruled out the participation of a silicate in the transmetalation. They predicted I–F exchange in $CH_2{=}CH{-}[PdIL_2]$ ($L = PMe_3$) to give $CH_2{=}CH{-}[PdFL_2]$. A coordination of the C=C bond of $CH_2{=}CH{-}SiMe_3$ to the palladium(II) center led to $CH_2{=}CH{-}[PdF(\eta^2\text{-}CH{=}CH{-}SiMe_3)L]$.[2c] The transmetalation would then occur from the latter in an unimolecular process. A nucleophilic attack of F^- onto the Si center of the coordinated $CH{=}CH{-}SiMe_3$ in $CH_2{=}CH{-}[PdI(\eta^2\text{-}CH{=}CH{-}SiMe_3)L]$ favoring the intramolecular transmetalation was also examined. Those two pathways are quite unlikely with $Ar'Si(OR)_3$ reagents because of the improbable coordination of the latter onto a palladium(II) center. A mechanism has been proposed for the reaction of the silanols $RSi(OH)Me_2$ with ArI, promoted by F^-, in which a first-order dependence was found for F^- at low concentrations and an inverse-order reaction at high concentrations. The authors proposed two different pathways towards the fluoride-activated disiloxane $[RSi(Me)_2(F)OSi(Me)_2R]^-$ which is involved in a transmetalation with [ArPdI].[3b]

We recently established that fluoride ions are involved in two kinetically antagonistic effects in Suzuki–Miyaura reactions: F^- is required to generate *trans*-$[ArPdFL_2]$ [Eq. (1)]

$$trans\text{-}[ArPdXL_2] + F^- \overset{K_X}{\rightleftarrows} trans\text{-}[ArPdFL_2] + X^- \qquad (1)$$

which reacts with $Ar'B(OH)_2$ in the rate-determining transmetalation (Scheme 2).[4a] However, at too high a concentration, F^- inhibits the reaction by competitive formation of the unreactive $Ar'B(OH)_{3-n}F_n^-$ ($n = 1$–3). Moreover, F^- promotes the reductive elimination from *trans*-$[ArPdAr'L_2]$, thus making this reaction faster than the transmetalation, which becomes rate determining (Scheme 2). The rate of the overall reaction performed with *trans*-$[ArPdXL_2]$ is thus controlled by the $[F]^-/[Ar'B(OH)_2]$ ratio.[4]

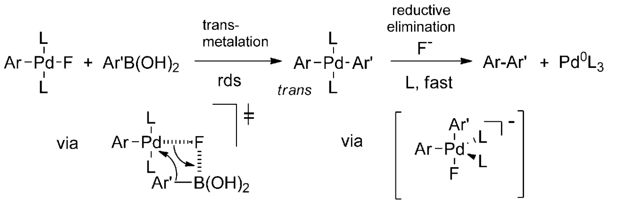

Scheme 2. Mechanism of the transmetalation/reductive elimination in the Suzuki–Miyaura reaction performed in the presence of nBu_4NF.[4] rds = rate-determining step.

We report herein the kinetic and mechanistic data aimed to understand the role of fluoride anions in Hiyama reactions performed with $PhSi(OMe)_3$ (**1**). Three roles for F^- were discovered, including the transmetalation of $[ArPdF(PPh_3)_2]$ with $Ar'Si(OMe)_3$.

Fluoride ions react with *trans*-$[ArPdX(PPh_3)_2]$[4a] to form *trans*-$[ArPdF(PPh_3)_2]$ [Eq. (1)].[4a,5] The isolated *trans*-[p-CNC_6H_4-Pd-$F(PPh_3)_2$] (**2**)[4a] ($C_0 = 2$ mM) was first submitted to a reaction with $PhSi(OMe)_3$ (**1**) in DMF at 25 °C. The reaction was performed in the presence of PPh_3 (2 equiv) to afford the stable and thus detectable $[Pd^0(PPh_3)_3]$ (**5**). The reaction was monitored by cyclic voltammetry (CV). The reduction peak R_1 of **2** ($E^p_{R1} = -1.95$ V vs SCE, Figure 1 a), whose peak current was proportional to its concentration,

---

[*] Dr. C. Amatore, Dr. L. Grimaud, Dr. G. Le Duc, Dr. A. Jutand
Ecole Normale Supérieure-PSL Research University
Département de Chimie, Sorbonne Universités
UPMC Univ Paris 06, CNRS UMR 8640 PASTEUR
24 Rue Lhomond, 75231 Paris Cedex 5 (France)
E-mail: christian.amatore@ens.fr
Anny.Jutand@ens.fr

[**] CNRS, ENS, and UPMC are thanked for financial support.

Supporting information for this article is available on the WWW under http://dx.doi.org/10.1002/anie.201400956.

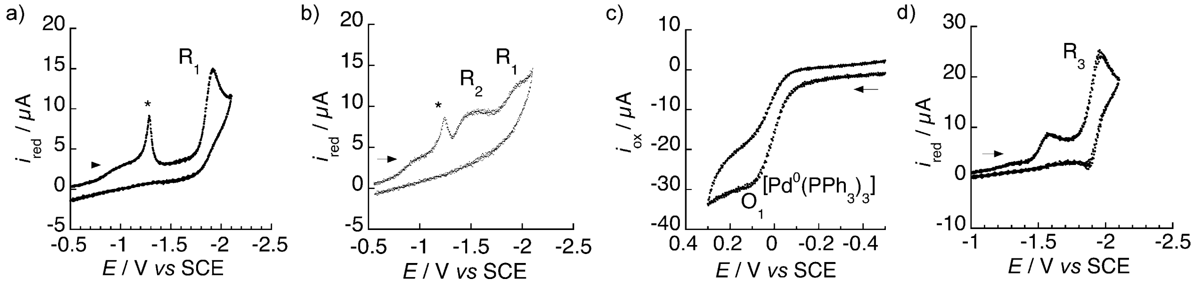

Figure 1. Cyclic voltammetry performed in DMF containing $n\mathrm{Bu_4NBF_4}$ (0.3 M) in the presence of $\mathrm{PPh_3}$ (4 mM) at a gold disk electrode ($d = 2$ mm) at the scan rate of 0.5 $\mathrm{Vs^{-1}}$, at 25 °C. a) Reduction at R_1 of *trans*-[p-$\mathrm{CNC_6H_4}$-Pd-F($\mathrm{PPh_3}$)$_2$] **2** (2 mM). b) 30 min after addition of PhSi(OMe)$_3$ (**1**; $\beta = 30$ equiv versus **2**) to **2**: reduction of *trans*-[p-$\mathrm{CNC_6H_4}$-Pd-Ph($\mathrm{PPh_3}$)$_2$] (**3**) at R_2. c) Oxidation at O_1 of [Pd^0($\mathrm{PPh_3}$)$_3$] (**5**) formed after addition of $\mathrm{F^-}$ ($\alpha = 40$ equiv versus **2**) to **3** after 20 min. d) Reduction at R_3 of p-$\mathrm{CNC_6H_4}$-Ph (**4**) formed together with **5** under the reaction conditions described for Figure 1 c after 22 min. * = Adsorption peak.

progressively disappeared in the presence of **1** ([**1**] $= \beta C_0$, $\beta = 30$ equiv), thus leading to the intermediate palladium(II) complex *trans*-[p-$\mathrm{CNC_6H_4}$-Pd-Ph($\mathrm{PPh_3}$)$_2$] (**3**) characterized by its reduction peak R_2 ($E^{\mathrm{p}}_{\mathrm{R2}} = -1.47$ V vs SCE) (Figure 1 b). The same complex was formed in our previous work when **2** was reacted with PhB(OH)$_2$.[4,6] However, the reaction of **2** with **1** was much slower than that of PhB(OH)$_2$ at identical concentrations.[4] It is only after addition of $n\mathrm{Bu_4NF}$ ([$\mathrm{F^-}$] $= \alpha C_0$, $\alpha = 40$ equiv, from a stock solution 1M in THF) that the intermediate complex **3** disappeared and the solution turned to yellow, thus leading to p-$\mathrm{CNC_6H_4Ph}$ (**4**) (99 %) and [Pd^0($\mathrm{PPh_3}$)$_3$] (**5**) (96 %). The compound **4** was characterized by its reduction peak at −2.0 V (R_3, reversible) and **5** by its oxidation peak at +0.05 V (O_1) (Figures 1 c,d). Their yield was determined from the increase of their respective current after addition of a known amount of the authentic samples **4** and **5**.

These results establish for the first time that *trans*-[ArPdFL$_2$] undergoes transmetalation with **1** at 25 °C as a consequence of the fluorophilicity of the silicon atom (Scheme 3). Moreover, as already proved in our previous work, $\mathrm{F^-}$ ions promote the reductive elimination from the stable *trans*-[ArPdAr′L$_2$] (Scheme 3).[4,7]

In contrast to **2**, the cyclic voltammetry showed that *trans*-[p-$\mathrm{CNC_6H_4}$-Pd-Br($\mathrm{PPh_3}$)$_2$] (**6**; $C_0 = 2$ mM in DMF, characterized by its reduction peak at −1.83 V vs SCE) did not react with **1** (from $\beta = 10$ to 50 equiv versus **6**) in the presence of 2 equivalents of $\mathrm{PPh_3}$ at 25 °C. The compounds **4** and **5** were not formed in the presence of $\mathrm{F^-}$ ($\alpha = 25$ equiv versus **6** for $\beta = 30$) at room temperature (see below). Conversely, a reaction took place at 70 °C and it delivered the cross-coupling product **4** as well as **5**. The role of $\mathrm{F^-}$ in the reaction shown in Scheme 4 could thus be investigated. With four $\mathrm{PPh_3}$ units per palladium center, those reaction conditions mimicked a Hiyama reaction catalyzed by [Pd^0($\mathrm{PPh_3}$)$_4$].[1]

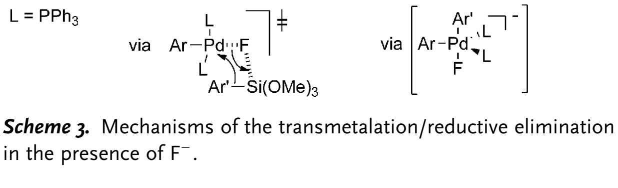

Scheme 3. Mechanisms of the transmetalation/reductive elimination in the presence of $\mathrm{F^-}$.

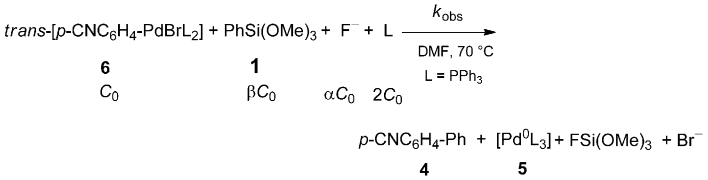

Scheme 4. Model reaction.

The kinetics of the formation of **5** was monitored by chronoamperometry at a rotating gold disk electrode polarized at +0.1 V (oxidation potential of **5** in DMF). The increase of the oxidation current of **5** (proportional to its concentration) was recorded with time just after addition of $n\mathrm{Bu_4NF}$ ($\alpha = 25$ equiv) to a solution containing **6** ($C_0 = 2$ mM), **1** ($\beta = 30$ equiv), and $\mathrm{PPh_3}$ (2 equiv) at 70 °C (Figure 2 a). The plot of ln$x$ versus time was linear (Figure 2 b; $x = (i_{\mathrm{lim}} - i_t)/i_{\mathrm{lim}}$ where i_{lim} = final oxidation current of **5**; i_t = oxidation current of **5** at time t). The value of k_{obs}, $1.4 \times 10^{-3}\ \mathrm{s^{-1}}$ (DMF, 70 °C), was determined from the slope of the linear correlation (Figure 2 b). At the end of the reaction, **5** and **4** were formed

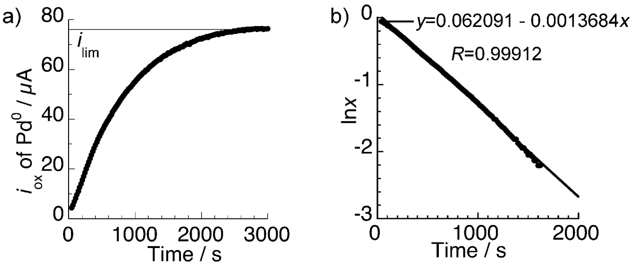

Figure 2. Kinetics of the reaction of *trans*-[p-$\mathrm{CNC_6H_4}$-Pd-Br($\mathrm{PPh_3}$)$_2$] (**6**; $C_0 = 2$ mM) with **1** ($\beta = 30$ equiv versus **6**) in the presence of $\mathrm{PPh_3}$ (2 equiv) and $n\mathrm{Bu_4NF}$ ($\alpha = 25$ equiv versus **6**) in DMF at 70 °C. a) Evolution of the oxidation current of **5** (proportional to its concentration) measured by chronoamperometry at a rotating gold disk electrode ($d = 2$ mm) polarized at +0.1 V vs SCE. b) Variation of ln$x$ vs time (see text for the definition of x).

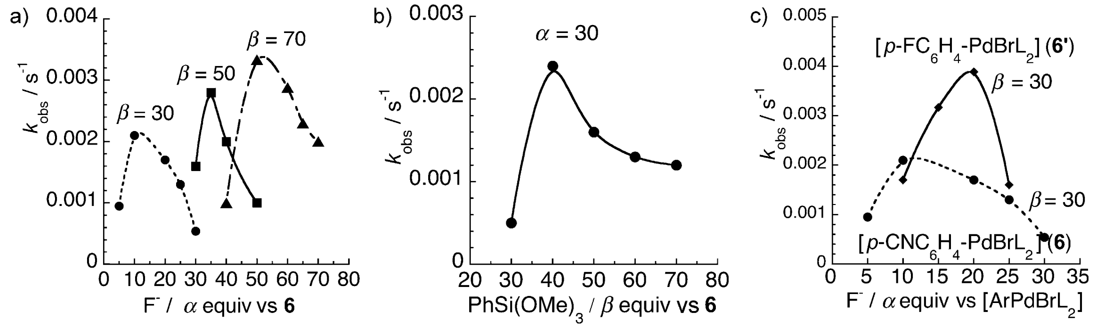

Figure 3. Reaction of **6** (2 mM) with **1** in the presence of F⁻ (α equiv versus **6**) and PPh$_3$ (2 equiv) in DMF at 70°C. a) Plot of the pseudo-first-order rate constant k_{obs} versus F⁻ (α equiv versus **6**) in the presence of **1** ($\beta = 30$, 50 and 70 equiv versus **6**). b) Plot of k_{obs} versus **1** (β equiv versus **6**) in the presence of F⁻ ($\alpha = 30$ equiv versus **6**). c) Plot of k_{obs} vs F⁻ (α equiv) for the reaction of **1** ($\beta = 30$ equiv) with **6** and *trans*-[p-FC$_6$H$_4$-Pd-Br(PPh$_3$)$_2$] **6'**.

in 97 and 98% yield respectively (see Figure S1a,b in the Supporting Information).

The plots of k_{obs} versus F⁻ concentration (α equiv versus **6**) exhibited a maximum regardless of the concentration of **1** (Figure 3a). The dependence of k_{obs} versus the concentrations of F⁻ and **1** revealed that k_{obs} characterized the rate of the transmetalation, which was rate-determining, with a subsequent faster reductive elimination. The plot of k_{obs} versus the concentration of **1** at constant F⁻ concentration also exhibited a maximum (Figure 3b). The fluoride was required to let the transmetalation proceed, but the reaction became slower when the concentration of **1** was too high and greatly exceeded that of F⁻ (Figure 3b). This result means that at an excess of **1**, F⁻ is quenched by **1** to form an unreactive species, the aryl silicate [PhSiF(OMe)$_3$]⁻ [Eq. (2)]. The affinity of F⁻ for silicon centers is indeed well known.[8]

Therefore, the bell-shaped curves of Figure 3a,b indicate that fluoride ions led to two kinetically antagonistic effects because F⁻ is involved in two competitive equilibriums (Scheme 5): one delivers the reactive *trans*-[ArPdF(PPh$_3$)$_2$] which reacts with Ar'Si(OMe)$_3$ in the rate-determining transmetalation; the second one delivers the unreactive silicate Ar'SiF(OMe)$_3$⁻. As for the Suzuki–Miyaura reaction,[4a] for $\beta > 30$ the maximum value of k_{obs} under each of the reaction conditions was observed for $\alpha/\beta = [F^-]/[PhSi(OMe)_3]$ values in the range 0.7–0.8, that is, less than unity (see Figure S2 in the Supporting Information). A bell-shaped plot of k_{obs} versus F⁻ concentration was also observed for another complex **6'** though with different α values for the same β value (Figure 3c).

$$Ar'Si(OMe)_3 + F^- \overset{K_F}{\rightleftharpoons} \underset{\text{unreactive}}{Ar'SiF(OMe)_3^-} \qquad (2)$$

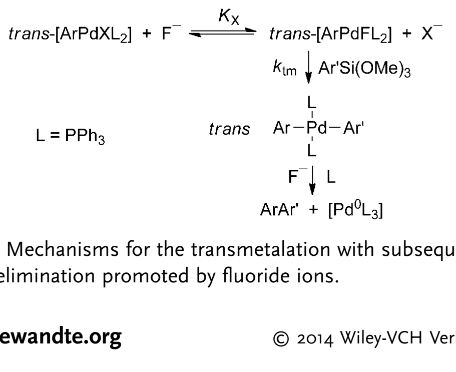

Scheme 5. Mechanisms for the transmetalation with subsequent reductive elimination promoted by fluoride ions.

The kinetic laws for the mechanism in Scheme 5 are expressed in Equations (3) and (4).[9]

$$\text{rate} = k_{obs}\,[Pd^{II}]_{total} \qquad (3)$$

$$k_{obs} = k_{tm}\beta C_0 \left(\frac{1}{1 + K_F[F^-]}\right)\left(\frac{K_X[F^-]}{[X^-] + K_X[F^-]}\right) \qquad (4)$$

When $[F^-] \ll 1/K_F$ and $[F^-] \ll C_0/(2K_X)$, then $k_{obs} \rightarrow 2k_{tm}\beta K_X[F^-]$, and k_{obs} increases linearly with [F⁻] at low concentrations. Conversely, when $[F^-] \gg 1/K_F$ and $[F^-] \gg C_0/(2K_X)$, then $k_{obs} \rightarrow k_{tm}\beta C_0/(K_F[F^-])$ and k_{obs} decreases hyperbolically with [F⁻] at high concentrations of [F⁻]. The theoretical variation of k_{obs} versus [F⁻] passes through a maximum, and is in agreement with the experimental observations (Figure 3a).

As stated above, the reaction in Scheme 4 did not work at 25°C regardless of the α/β ratio (0.5, 0.75). Neither **5** nor ArAr' were formed. However, another reaction took place, thus affording the new complex **7**, which is characterized by its reduction peak at −2.17 V (see Figure S3 in the Supporting Information). The addition of F⁻ ($\alpha = 5$ equiv) to **6** (2 mM) partly generated **2** [Eq. (1)]. This step was clearly observed by CV where the reduction peaks R$_1$ and R$_2$ of **2** and **6**, respectively, coexisted. Both disappeared ultimately in the absence or presence of **1**, thus leading to the new complex **7**. The ^{31}P NMR analysis of the solutions exhibited a major singlet at $\delta = 31.77$ ppm as is observed for the dimer **7** which is generated by reacting [p-CNC$_6$H$_4$-Pd(μ-I)(PPh$_3$)]$_2$ with nBu$_4$NF (20 equiv) (see Figure S4 in the Supporting Information).[4a,5]

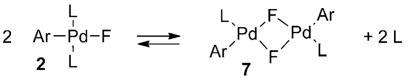

(5)

Ar = p-CNC$_6$H$_4$, L = PPh$_3$

The compound **7** was not formed when the isolated **2** was reacted with **1** in the presence of PPh$_3$ (2 equiv) at room temperature (see Scheme 3). But it was formed from **6** in the presence of F⁻, **1**, and PPh$_3$ (2 equiv) at room temperature.

This difference presumably derives from the low thermodynamic concentration of $[ArPdF(PPh_3)_2]$, when starting from **6**, which did not allow a fast transmetalation and thus, all the aryl/Pd^{II} were converted into the unreactive dimer **7** [Eq. (5)]. Upon increasing the temperature, the reaction of **1** with $[ArPdF(PPh_3)_2]$, thus leading to ArAr′ and **5**, became faster and the formation of **7** in Equation (5) was by-passed.

Two other putative pathways have been ruled out. When the preformed silicate $[PhSiF(OMe)_3]^-$ (10 equiv) was added to a solution of **6** (2 mM) and PPh_3 (2 equiv) at 25 °C, **6** disappeared, but neither ArAr' nor **5** were formed. Only the dimer **7** was detected by its reduction peak at −2.17 V. Consequently, the silicate $[PhSiF(OMe)_3]^-$ did not react with **6** at 25 °C. However, the formation of **7** attested that some transient $[ArPdF(PPh_3)_2]$ was generated (experimentally observed; see the Supporting Information) by the reaction of **6** with F^- [Eq. (1)], the latter being released from $[PhSiF(OMe)_3]^-$ in its equilibrium with **1** [Eq. (2)]. This evidence suggests that the affinity of **6** for F^- is higher than that of **1** at comparable concentrations.

On the other hand, addition of the preformed $[PhSiF(OMe)_3]^-$ (10 equiv) to a solution of **2** (2 mM) in the presence of PPh_3 (2 equiv) at 25 °C delivered the coupling product **4** (42 %) and **5**, but in a slow reaction (80 min), much slower than that of **1** at the same concentration at 25 °C because the reaction proceeded via **1**, which was generated at low thermodynamic concentration in its equilibrium with $[PhSiF(OMe)_3]^-$ [Eq. (2)]. This result is in agreement with the slow reactions observed from **6** at high fluoride concentrations where both $[PhSiF(OMe)_3]^-$ and **2** were the major species (Figure 3 a).

Consequently, the most efficient pathway for the transmetalation is the reaction of *trans*-$[ArPdF(PPh_3)_2]$ with $Ar'Si(OMe)_3$, a reaction which even takes place at room temperature. The three roles of F^- in the Hiyama reactions are displayed in Scheme 6.

In conclusion, the three mechanistic roles of fluoride ions in Hiyama reactions involving $Ar'Si(OMe)_3$ have been established. The crucial step is the formation of *trans*-$[ArPdF(PPh_3)_2]$, which reacts with $Ar'Si(OMe)_3$ in a rate-determining transmetalation step, whereas the silicate $[Ar'SiF(OMe)_3]^-$ is not reactive. This process leads to two antagonistic roles of F^- and the rate of the overall reaction is controlled by the ratio $[F^-]/[Ar'Si(OMe)_3]$, which must be less than unity. A third role exerted by F^- is the promotion of the reductive elimination from *trans*-$[ArPdAr'(PPh_3)_2]$, as was already established in the Suzuki–Miyaura coupling.[4] The overall reactions starting from *trans*-$[ArPdBr(PPh_3)_2]$ in the Hiyama reactions are much slower than those in Suzuki–Miyaura reactions at the same concentration of reagents and F^- since the former do not take place at 25 °C. This study explains why arylboronic acids can react with aryl iodides or bromides at room temperature, whereas arylsilanes require higher temperatures.[1,2]

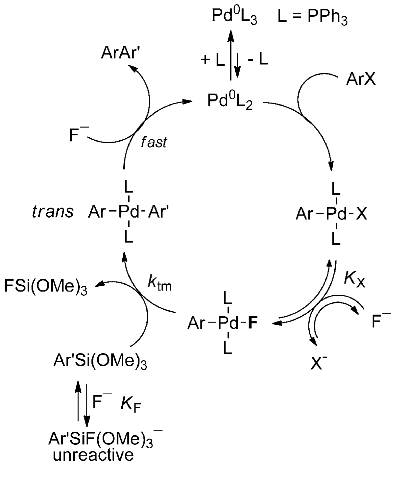

Scheme 6. Mechanism of the Hiyama reaction performed in the presence of fluoride anions (nBu_4NF) at 70 °C.

Received: January 28, 2014
Revised: March 14, 2014

Keywords: cross-coupling · fluoride · kinetics · palladium · reaction mechanisms

[1] a) Y. Hatanaka, T. Hiyama, *Tetrahedron Lett.* **1988**, *29*, 97–98; b) K.-i. Gouda, E. Hagiwara, Y. Hatanaka, T. Hiyama, *J. Org. Chem.* **1996**, *61*, 7232–7233; c) K. Shibata, K. Miyazawa, Y. Goto, *Chem. Commun.* **1997**, 1309–1310; d) E. Mowery, P. DeShong, *Org. Lett.* **1999**, *1*, 2137–2140; e) H. M. Lee, S. P. Nolan, *Org. Lett.* **2000**, *2*, 2053–2055; f) G. A. Molander, L. Iannazzo, *J. Org. Chem.* **2011**, *76*, 9182–9187; g) Y. Hatanaka, T. Hiyama, *Synlett* **1991**, 845–853; h) T. Hiyama, E. Shirakawa, *Organosilicon Compounds in Topics in Current Chemistry*, *Vol. 219*, Springer, Berlin **2002**, pp. 61–85.

[2] a) Y. Hatanaka, K.-i. Goda, Y. Okahara, T. Hiyama, *Tetrahedron* **1994**, *50*, 8301–8316; b) Y. Hatanaka, T. Hiyama, *J. Am. Chem. Soc.* **1990**, *112*, 7793–7794; c) A. Sugiyama, Y.-y. Ohnishi, M. Nakaoka, Y. Nakao, H. Sato, S. Sakaki, Y. Nakao, T. Hiyama, *J. Am. Chem. Soc.* **2008**, *130*, 12975–12985.

[3] a) S. E. Denmark, D. Wehrli, *Org. Lett.* **2000**, *2*, 565–568; b) S. E. Denmark, R. F. Sweis, D. Wehrli, *J. Am. Chem. Soc.* **2004**, *126*, 4865–4875; c) S. E. Denmark, C. Regens, *Acc. Chem. Res.* **2008**, *41*, 1486–1499; d) S. E. Denmark, J. H. C. Liu, *Angew. Chem.* **2010**, *122*, 3040–3049; *Angew. Chem. Int. Ed.* **2010**, *49*, 2978–2986.

[4] a) C. Amatore, A. Jutand, G. Le Duc, *Angew. Chem.* **2012**, *124*, 2542–2545; *Angew. Chem. Int. Ed.* **2012**, *51*, 2492–2503; b) C. Amatore, A. Jutand, G. Le Duc, *Chem. Eur. J.* **2013**, *19*, 10082–10093.

[5] For the synthesis of $[ArPdF(PPh_3)_2]$, see: M. C. Pilon, V. V. Grushin, *Organometallics* **1998**, *17*, 1774–1781.

[6] For the characterization of *trans*-$[ArPdAr'(PPh_3)_2]$, see: C. Adamo, C. Amatore, I. Ciofini, A. Jutand, H. Lakmini, *J. Am. Chem. Soc.* **2006**, *128*, 6829–6836.

[7] For reductive elimination induced by a fifth ligand in square-planar d^{10} complexes, see: a) R. Giovannini, P. Knochel, *J. Am. Chem. Soc.* **1998**, *120*, 11186–11187; b) A. G. Jarvis Amanda, I. J. S. Fairlamb, *Curr. Org. Chem.* **2011**, *15*, 3175–3196.

[8] K. C. Kumara Swany, V. Chandrasekhar, J. J. Harland, J. M. Holmes, R. O. Day, R. R. Holmes, *J. Am. Chem. Soc.* **1990**, *112*, 2341–2348.

[9] For similar equations in the Suzuki–Miyaura reactions performed in the presence of F^-, see Ref. [4].